Demonstration of a stable, high-performance Mach-Zehnder Polarization-Insensitive Fiber Optical Parametric Amplifier

F. Bessin[1, 2], V. Gordienko[1], F. M. Ferreira[3], and N. J. Doran[1]
(1) Aston Institute of Photonic Technologies, Aston University, Birmingham, B4 7ET, UK
(2) Now with Univ Angers, LPHIA, SFR MATRIX, F-49000 Angers, France
(3) Optical Networks Group, University College London, London, WC1E 6BT, UK
florent.bessin@univ-angers.fr

Abstract: We demonstrate a Mach-Zehnder architecture for polarization-insensitive fiber optical parametric amplifiers to obtain a noise figure of ~4.5dB and reduction of nonlinear crosstalk as compared to previously demonstrated PI-FOPAs while demonstrating net gain up to 24dB.

1. Introduction

In the last decades, fiber optical parametric amplifiers (FOPA) have gained a significant attention as a promising technology for amplifying signals with high gain, low-noise figure, and on theoretically unconstrained operation wavelength ranges [1]. Despite their advantages over more traditional optical amplifiers such as Erbium-doped fiber amplifiers (EDFAs), FOPAs also have limitations, such as polarization dependent gain (PDG) that remains an issue for practical applications. Nevertheless, during the last decade this issue was overcome with a looped polarization-insensitive FOPA (PI-FOPA) [2]. For example, this architecture has enabled PI-FOPA employment in multi-span transmission experiments [3], and PI-FOPA operation across a continuous band of 35 nm [4]. In looped PI-FOPA an arbitrary polarized signal is split into two orthogonally polarized components that are amplified independently and propagate in opposite directions inside a loop. Since signal components are amplified independently the looped PI-FOPA is made of two highly nonlinear fiber (HNLF) sections, each amplifying only one signal component. Consequently, each of these components must go through an additional section of HNLF after amplification leading to significant nonlinear crosstalk, or before amplification, leading to noise figure degradation [5].

Our new PI-FOPA based on a Mach-Zehnder (MZ) architecture [6] overcomes this issue. Unlike looped PI-FOPA, each polarization component in MZ-FOPA propagates through only one arm of the MZ and then polarization components are recombined thus avoiding aggravation of NF and nonlinear crosstalk. This configuration is employed by PI optical parametric amplifiers based on periodically poled Lithium Niobate [7], but we are the first to employ it in FOPAs and to overcome the challenge of optical path matching in such a long nonlinear MZ arrangement.

In this paper we present a PI-FOPA based on MZ architecture and employ it to amplify a grid of wavelength division multiplexed (WDM) channels including a 100G PM-QPSK signal. We demonstrate that the MZ-FOPA enables the lowest to the best of our knowledge PI-FOPA noise figure of 4.5 dB along with an improved nonlinear crosstalk tolerance as compared to looped PI-FOPA. We compare BER of signals amplified by the MZ-FOPA and a commercial EDFA and confirm the MZ-FOPA stability and feasibility for signal amplification.

2. Experimental Setup

Fig. 1(a) shows the experimental setup used to characterize a MZ-FOPA in terms of NF and BER when amplifying a set of WDM signals with varied power. The setup includes a WDM signals emulator (green box), MZ-FOPA (yellow box) under test, a net gain and NF measurement setup (red box), and a WDM signals receiver (blue box).

The WDM signals emulator generated 17x100 GHz-spaced WDM channels between 1528.0 nm and 1540.56 nm. One of channels was a 35 Gbaud PM-QPSK signal (100G) sourced from a Ciena transponder Wavelogic 3 (Tx). Its wavelength was adjusted across the WDM range for BER measurements. Other channels were sourced from an amplified spontaneous emission (ASE) source and then shaped and combined with the 100G signal by a programmable filter (WSS). The power per channel was tuned by an EDFA and a variable optical attenuator (VOA).

The receiver coupled the amplified signals with ASE noise *via* a 90/10 coupler to tune the optical signal-to-noise ratio. Then, the 100G channel was passed through a band pass filter (BPF) and coherently detected by the Ciena transponder Wavelogic 3 (Rx). The signal BER was measured *via* error counting.

The MZ-FOPA is highlighted by a yellow box in Fig. 1(a). In this amplifier the amplified signal is split into two polarization components *via* a polarization beam splitter (PBS1). Each polarization component is then independently amplified through a four-wave-mixing (FWM) process with a co-propagating pump ($\lambda_{pump} = 1553.33$ nm) in a ~100 m long HNLF ($\lambda_0 \sim 1551$ nm, $\gamma \sim 14$ W^{-1}.km^{-1}). Pumps are coupled to and decoupled from the HNLFs *via*

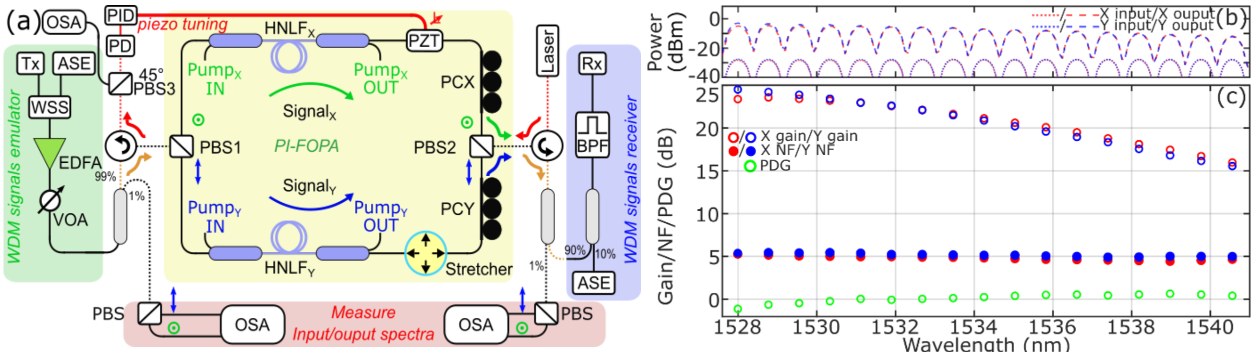

Fig. 1. (a) Experimental setup to evaluate performance of a MZ-FOPA (yellow box). PID: proportional-integrate-derivative. (b) WDM signal input/output spectra for X/Y polarization components. (c) Net gain, PDG, and NF for each channel.

200 GHz-wide WDM filters (blue components in Fig. 1(a)) centered at 1553.33 nm. The amplified polarization components are then recombined through PBS2. Alignment of the polarization components with the axes of PBS2 is achieved with electronically addressable polarization controllers (PCX/PCY). A feedback loop was used to tune PCX/PCY plates in real-time by maximizing/stabilizing the FOPA output power *via* a steepest descent algorithm.

In looped PI-FOPA both polarization components follow intrinsically the same optical path, but in MZ-FOPA polarization components follow different paths. The optical path difference causes a delay between polarization components which might result in high polarization mode dispersion (PMD) for signal. We minimize the delay between polarization components by matching the optical path length of the two MZ arms with a difference < 0.2 mm (delay of $\sim$1 ps) by using a fiber stretcher in the shortest arm. We used the interferometric nature of the MZ-FOPA to set the stretcher very accurately to the right position. For this purpose, we added a pair of circulators like in Ref. [8], one at each side of MZ-FOPA, allowing us to propagate in opposite directions the amplified polarization components and a probe beam without interference between them. By maintaining the polarization state of this probe beam at its output from MZ-FOPA and using PBS3 with polarization axis at 45° from those of PBS1, we observed the interferometric behavior of the probe beam with a high visibility. This interferometric signal was both recorded by a photodetector (PD) and an optical spectrum analyzer (OSA). We measured from optical interference spectra the free spectral range ($FSR = c/(n\,\Delta L)$, with ΔL the difference of optical path between the MZ arms) and set it to a value $\sim$ 1 THz by tuning the fiber stretcher, hence ΔL~0.2 mm and delay $\sim$ 1 ps, far lower than the PMD tolerance of $\sim$150 ps of the Ciena receiver. The interference signal detected by the PD was used as an error signal for a feedback loop system that drives a piezo-electric fiber stretcher (PZT) added in arm X to compensate for length fluctuations.

Finally, we want to highlight that dotted lines in Fig. 1(a) correspond to polarization maintaining (PM) fibers, thus adding calibrated 1% PM tap coupler and PBS at MZ-FOPA input and output, we could record input and output spectra and performed for both polarization components and each channel measurements of net gain and NF.

3. Experimental Results and Discussion

Fig. 1(b) shows an example of WDM signal spectra (for both polarization components) at input/output of MZ-FOPA for input power of -28 dBm per channel. The corresponding net gain spectra for both polarization components and each channel are depicted in Fig. 1(c) by red and blue empty circles. A net gain >15.5 dB and up to 24 dB was measured across the range of 12.5 nm with a PDG < 1 dB (green circles). However, the measurements imply gain bandwidth is much larger spanning beyond our measurement range in the C band. Thus, MZ-FOPA should be capable to provide a gain bandwidth of at least 40 nm as demonstrated by a looped PI-FOPA [4] with a shorter gain fiber.

Fig. 1(c) also shows the corresponding optical NF measured for both polarization components for each channel depicted in Fig. 1(b) with filled circles. The optical NF was calculated for each channel using Eq. (1) (source subtraction method [9]), where N_{input} and N_{output} are the input and output noise powers respectively measured at each channel frequency when turning this channel off by the WSS. The parameters B_0, G, h and ν correspond to the OSA resolution bandwidth, net gain, Planck constant, and the 100G channel frequency respectively.

$$\mathrm{NF} = \frac{N_{output}}{G h \nu B_0} + \frac{1}{G} - \frac{N_{input}}{h \nu B_0} \qquad (1)$$

In Fig. 2(a-b), we show the NF obtained for channels at 1530.3, 1534.28, and 1537.40 nm versus the output power per channel while the input power per channel was varied from -44.8 to -17.3 dBm. We ensured during measurements that the net gain was constant (23 dB, 21 dB, and 18.5 dB respectively) for each channel and polarization component as input power was varied. For an output power per channel < -6 dBm, the unwanted FWM is negligible and FOPA operates in a linear regime, so the NF is essentially 3 dB plus insertion loss preceding the FOPA gain section. In this case the NF is in the range between 4.5 dB and 5.5 dB across all channels for both polarization components. For output

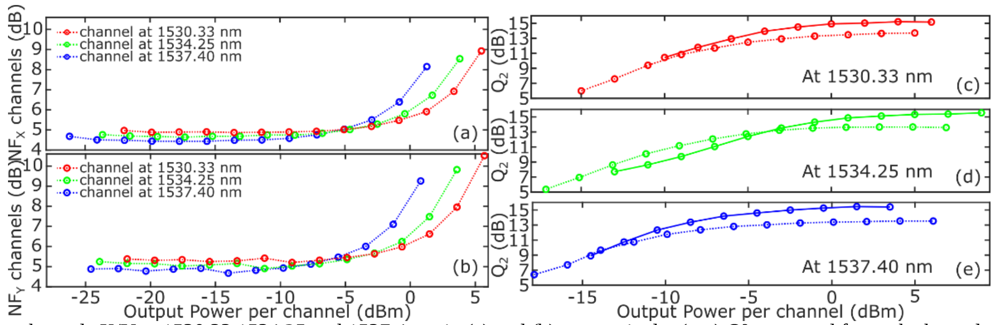

Fig. 2. NF for channels X/Y at 1530.33,1534.25 and 1537.4 nm in (a) and (b), respectively. (c-e) Q² measured for each channel with our MZ-FOPA (dotted lines) and a commercial EDFA (solid lines).

power per channel >-6 dBm the unwanted FWM leads to significant NF increase with signal power. The record low PI-FOPA NF of 4.5 dB is facilitated in MZ-FOPA by reduction of insertion loss as compared to looped PI-FOPAs. We also confirm improvement of nonlinear crosstalk tolerance as NF below 6 dB is maintained up to a total output power of ~10 dBm as compared to ~4 dBm in the looped PI-FOPA [5].

Fig. 2(c-e) shows the signal quality factor Q² derived from the BER measurements as WDM signal power is varied for three 100G signal wavelengths (1530.33, 1534.28, and 1537.40 nm) when the signal is amplified by MZ-FOPA (dotted line) and a commercial EDFA (solid line). Net gain of MZ-FOPA and EDFA was the same for each wavelength. The MZ-FOPA and a commercial EDFA show very close performance when output signal power is below -10…-5 dBm (depending on wavelength). This corresponds to the amplified signal quality factor Q^2 up to ~11 dB or BER of 2×10^{-4}. The Q^2 curves for the MZ-FOPA and the EDFA diverge with the signal power increase, whereas the former curve reaches a plateau at 13 dB and the latter at 15 dB. Although, an increase in MZ-FOPA noise figure at high output signal power contributes to the MZ-FOPA performance degradation in this range, the flat nature of the Q-factor curve implies that the MZ-FOPA performance is rather limited by the impact of the pump phase modulation [10] or PMD. However, the performance difference between the MZ-FOPA and the EDFA becomes notable at BER much higher than that typical for optical communications operation. Importantly, a similar investigation performed with low noise looped PI-FOPAs [5] showed a significant Q^2 decrease at output power per channel > 0 dBm due to nonlinear crosstalk. Therefore, our result confirms that the MZ architecture of PI-FOPA allows to mitigate nonlinear crosstalk as compared to looped PI-FOPAs while facilitating low noise figure too.

Conclusions

We demonstrate that Mach-Zehnder architecture allows amplification of WDM PDM-QAM signals in PI-FOPAs with low noise and low nonlinear crosstalk. We employ this architecture for amplification of 100G PDM-QPSK signal in a WDM environment and demonstrate net gain up to 24 dB, noise figure of 4.5-5.5 dB up to output power per channel of -5 dBm, and BER matching that of a commercial EDFA. This makes the Mach-Zehnder architecture the most suitable for design of high-performance PI-FOPAs.

Acknowledgement

We thank Dr S. Takasaka and Dr R. Sugizaki of Furukawa Electric for HNLFs, and Dr C. Laperle of Ciena for the transponder. This work was supported by H2020 MSCA (713694), UK EPSRC projects FPA-ROCS (EP/R024057/1) and EEMC (EP/S016171/1), and the UKRI Future Leaders Fellowship under Grant MR/T041218/1. Data underlying the results presented in this paper are available at: https://doi.org/10.17036/researchdata.aston.ac.uk.00000613.

References

[1] M. E. Marhic, *Fiber Optical Parametric Amplifiers, Oscillators and Related Devices* (Cambridge University Press, 2008).
[2] S. Takasaka *et al*, "Polarization insensitive fiber optical parametric amplifier using a SBS suppressed diversity loop," in OFC 2016, p. M3D.4.
[3] M. F. C. Stephens *et al*, "In-line and cascaded DWDM transmission using a 15dB net-gain polarization-insensitive fiber optical parametric amplifier," Opt. Express **25**, 24312-24325 (2017).
[4] C. B Gaur *et al*, "Polarization-insensitive fibre optic parametric amplifier with gain bandwidth of 35 nm in L-band," ECOC 2021, p. Tu2A.4.
[5] V. Gordienko *et al*, "Looped Polarization-Insensitive Fiber Optical Parametric Amplifiers for Broadband High Gain Applications", J. Light. Technol. **39**, 6045-6053 (2021).
[6] F. Bessin *et al*, "Mach-Zehnder FOPA for Dual Polarization Wavelength-Division-Multiplexed 100G Signal Amplification", CLEO 2022, p. SF3M.2.
[7] T. Kobayashi *et al*, "Wide-Band Inline-Amplified WDM Transmission Using PPLN-Based Optical Parametric Amplifier," J. Light. Technol. **39**, 787-794 (2021).
[8] F. Bessin *et al*, "Real-Time Characterization of Period-Doubling Dynamics in Uniform and Dispersion Oscillating Fiber Ring Cavities", Phys. Rev. X **9**, 041030 (2019).
[9] D. M. Baney *et al*, "Theory and Measurement Techniques for the Noise Figure of Optical Amplifiers", Opt. Fiber Technol. **6**, 122 (2000).
[10] M. Bastamova *et al*, "Impact of Pump Phase Modulation on Fibre Optical Parametric Amplifier Performance for 16-QAM Signal Amplification," in ECOC 2022, paper Tu5.6.